Electronic Supplementary Material (ESI) for Nanoscale.

Water-processable cellulose-based resist for advanced nanofabrication

*Camilla Dore[1], Johann Osmond[2] and Agustín Mihi[1]**

1 Institut de Ciència de Materials de Barcelona (ICMAB-CSIC), Campus de la UAB, 08193 Bellaterra, Catalonia, Spain

2 ICFO-The Institute of Photonic Sciences, Av. Carl Friedrich Gauss, 3, 08860 Castelldefels – Barcelona

*(corresponding author: *amihi@icmab.es)*

Supporting Information

Contents:

Section 1. Calculation of HPC film thickness

Hydroxypropyl cellulose (Mw=100000 KDa) was obtained from Sigma-Aldrich. Further information on the material can be found in the following link: https://www.sigmaaldrich.com/catalog/papers/22961411 .

The thickness of flat HPC films on silicon was extracted by fitting the experimental reflectivity with spectra calculated by the transfer matrix method.[30] The reflection spectrum from a thin film of the HPC shows characteristic oscillations (Fabry-Perot oscillations) which depend on the films thickness and dielectric constants of the layered materials. **Figure S1** shows both experimental (blue) and calculated (red) reflection spectra in the visible range for two exemplar HPC films with different thicknesses. The averaged refractive indexes used for the fittings are 1.47 for HPC[29] and 3.9 for silicon,[31] and the film thickness are set to 220 nm for the spectrum on the left and to 405 nm for the spectrum on the right. Experimental spectra were acquired using an FTIR spectroscope attached to a microscope with a 4X objective. Different spots of the samples have been probed, showing a high homogeneity of the HPC film.

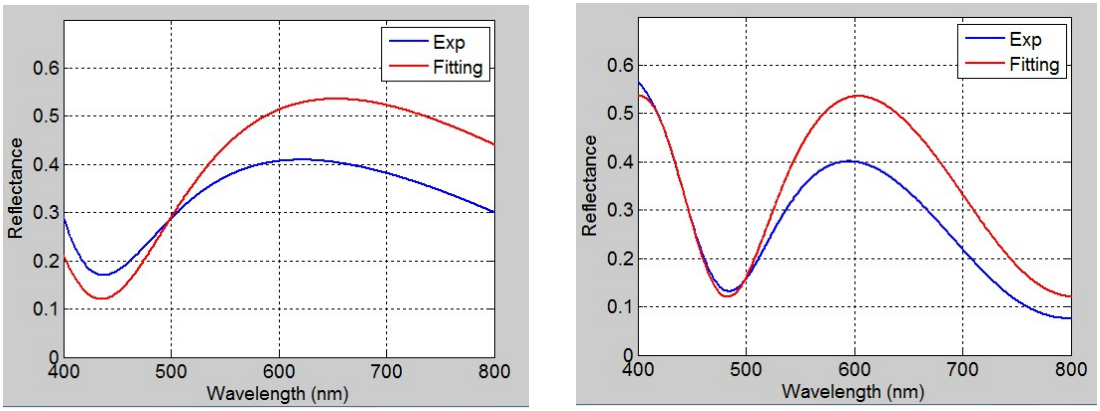

Figure S1: Experimental (blue) and calculated (red) reflection spectra for HPC films on silicon with thicknesses of 220 nm (left) and 405 nm (right).

Section 2. Depth of the imprinted features in HPC films

Atomic force microscopy analysis was performed in representative HPC films imprinted with holes and pillars with lattice parameter of 400 nm in order to measure the depth or height of the

imprinted features. Results are exhibited in **Figure S2**. The holes depth was approximately 365 nm while the pillars height was 362 nm. The estimate AFM error in the Z direction is ± 40 nm.

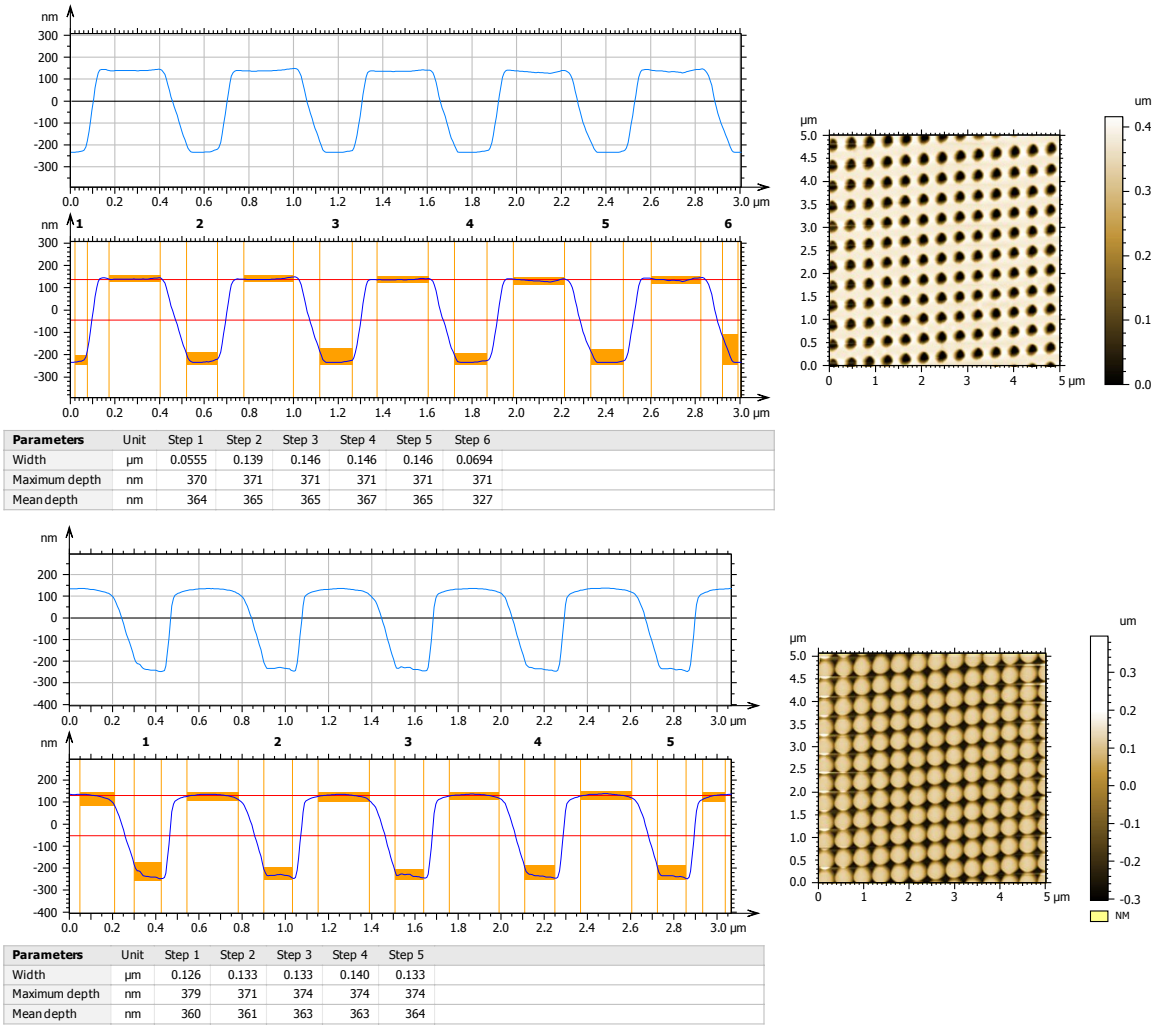

Parameters	Unit	Step 1	Step 2	Step 3	Step 4	Step 5	Step 6
Width	µm	0.0555	0.139	0.146	0.146	0.146	0.0694
Maximum depth	nm	370	371	371	371	371	371
Mean depth	nm	364	365	365	367	365	327

Parameters	Unit	Step 1	Step 2	Step 3	Step 4	Step 5
Width	µm	0.126	0.133	0.133	0.140	0.133
Maximum depth	nm	379	371	374	374	374
Mean depth	nm	360	361	363	363	364

Figure S2: representative HPC imprinted pillar and holes AFM measurements: Atomic force microscopy image and representative profiles with step height calculation for holes and pillars imprinted in HPC.

Section 3. Calculation of the Residual layer thickness

The resist volume equivalence model assumed to calculate the residual layer thickness is schematized in **Figure S3**. Once the PDMS mold features are filled with the HPC, the material flow stops and the initial HPC volume V_1 must be equal to the volume V_2 obtained after the HPC

patterning. The initial thickness h_i required to obtain a residual layer with thickness h_f equal to zero, can thus be calculated knowing the pattern geometry and the features depth h_r.

As an example we apply this model to one of the PDMS molds used in this work and consisting of a 1 cm^2 imprinted area of pillars in a square array with radius r=150 nm, pillars height h_r=350 nm and lattice parameter L= 400. Using the formulas and schemes depicted in **Figure S4**, the minimum initial layer thickness h_{min} required to fill the mold feature and ideally leaving no residual layer corresponds to 195 nm. Spin coated layers with thicknessess h_i above the calculated minimum thickness h_{min} will result in the formation of a residual layer with thickness $h_f = h_i - h_{min}$.

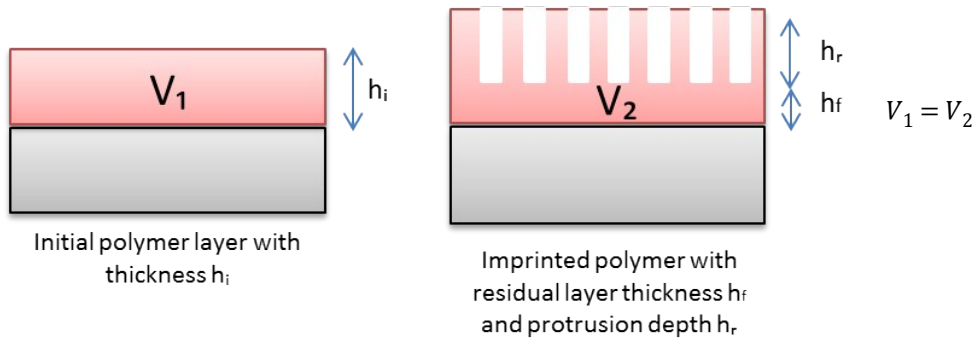

Figure S3: resist volume equivalence model: Schematic of volumes involved during HPC molding.

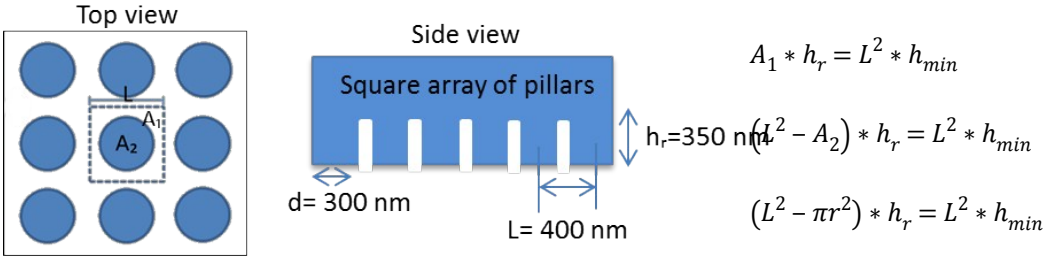

Figure S4: PDMS mold geometry: Top view and side view of the PDMS mold used and related minimum initial layer thickness calculation.

To verify experimentally this calculation we scratched the HPC film inside and outside the patterned area and we measured via atomic force microscopy the steps height. Outside the patter (**Figure S6**) we obtained an HPC layer thickness of 223 nm, consistent with previous optical measurements. Inside the pattern (**Figure S5**) we measured a film thickness of 381 nm. This

thickness represents the distance between the top of the imprinted feature and the underlying substrate. Considering that the holes depth is 350 nm, the residual layer thickness for this sample is 31 nm, which is quite close to the theoretically calculated one (28 nm).

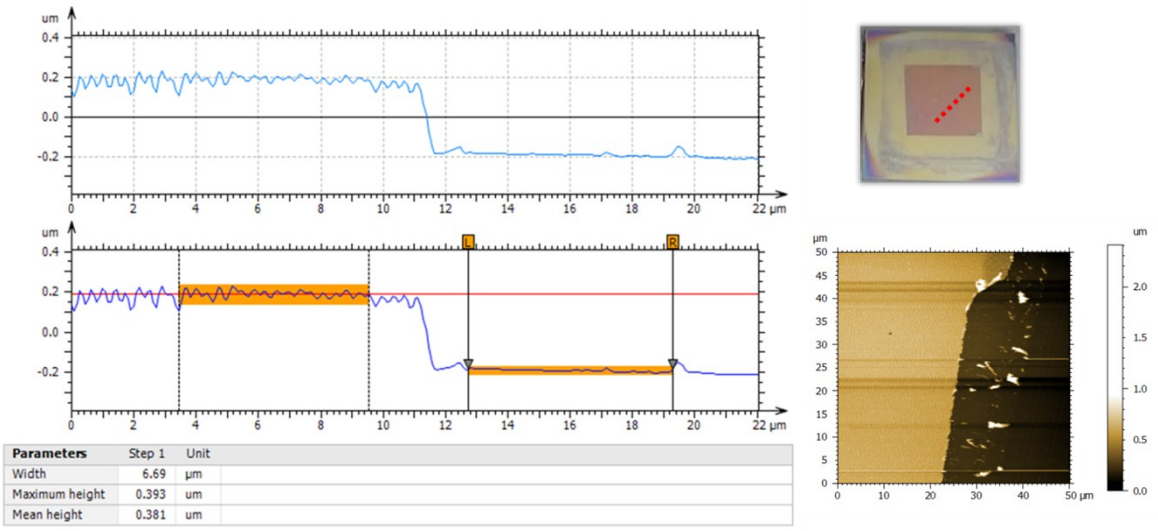

Figure S5: HPC thickness inside pattern: Atomic force microscopy image and representative profiles with step height of a scratched area inside the HPC patterned region (red dashed line in the sample photo).

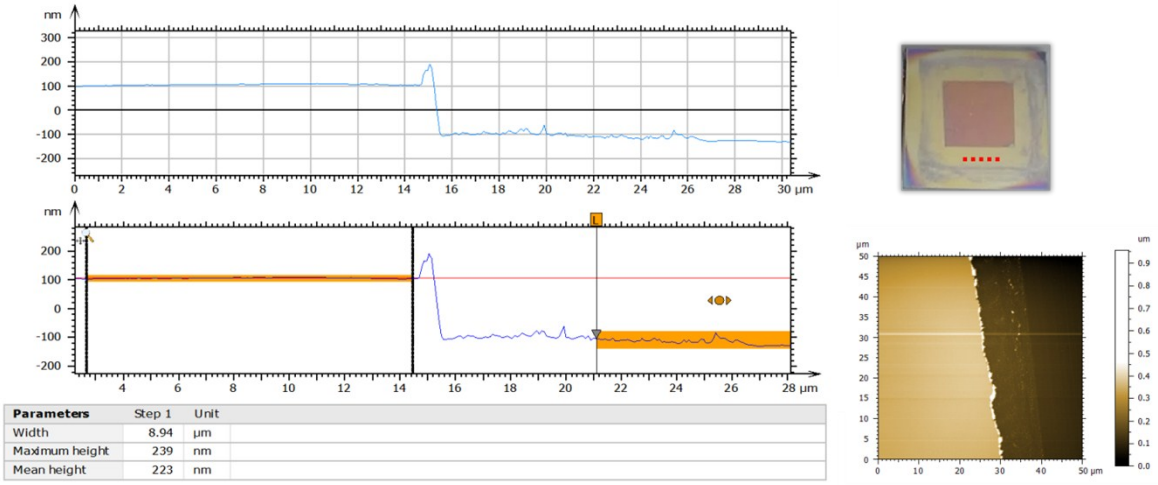

Figure S6: HPC thickness outside pattern: Atomic force microscopy image and representative profiles with step height of a scratched area outside the HPC patterned region (red dashed line in the sample photo).

Section 4. Calculation of the Reactive Ion Etching rates

In order to etch the residual layer of cellulose and to transfer the patter to the silicon wafer, we followed a pseudo Bosch etching process. In a pseudo Bosch etching a mixture of C_4F_8 and SF_6 gases is simultaneously injected in the RIE chamber. The ionization of C_4F_8 leads to the formation of a polymeric chain of CF_2 that settles on the substrate protecting it from erosion while substrate milling is carried out by the accelerated SFx and Fy ions impinging on the substrate. However, the DC bias accelerates the ions towards the target material and the passivation layer deposited on the horizontal surfaces is removed at a faster rate than the one deposited on the vertical side walls. As a result, with an appropriate tuning of the gas ratio and the ICP power, it is possible to achieve a dynamic equilibrium in which the Silicon vertical sidewalls are protected by the CF_2 polymer while the horizontal surfaces remains exposed to milling ions. Selectivity values (Etching rate Si/etching rate HPC) have been estimated testing five different set of etching parameters: i) 300 W ICP Fw (forward) power and 70 sccm C_4F_8 flow, ii) 300 W ICP Fw power and 80 sccm C_4F_8 flow, iii) 300 W ICP Fw power and 90 sccm C_4F_8 flow, iv) 400 W ICP Fw power and 70 sccm C_4F_8 flow, v) 300 W ICP Fw power and 90 sccm C_4F_8 flow. For all the experiment, pressure has been set to 15 mtorr, RF generator power to 35 W, SF_6 gas flow to 45 sccm.

Silicon and HPC etching rates shown in figure S7 have been calculated by the linear fit of etching depth for etching times of 1,2 and 3 min. (batches i, ii, iii) and for etching times 1 and 2 min. (batches iv, v). HPC thicknesses have been calculated by fitting the Fabry Perot oscillation as previously described. Measurements have been done on flat HPC areas outside the pattern, or using a flat layer of HPC with a known initial thickness as reference. Silicon holes depth has been measured with SEM cross section (figure S7).Data in the graphs were calculated in the following way:

- Etching rates HPC: [220 – (measured HPC thickness outside pattern)]/etching time
- Etching rate Silicon: (Holes depth)/[(time etching)-(time to remove residual layer)]
- Time to remove the residual layer: [(cellulose etching rate)*(residual layer thickness)] assuming a residual layer thickness of 25 nm.

Batch (i): *Fw power: 300 W, C_4F_8 flow: 70 sccm*

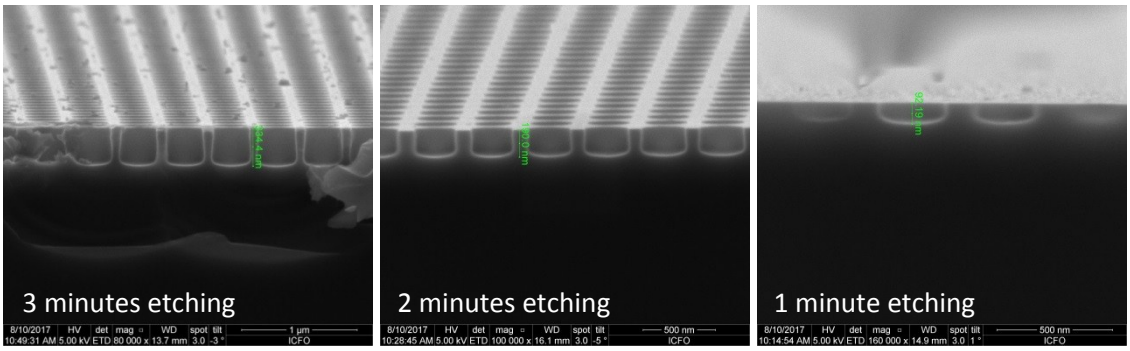

HPC etching rate

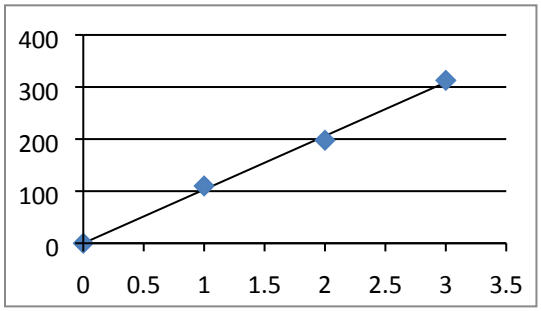

Silicon etching rate

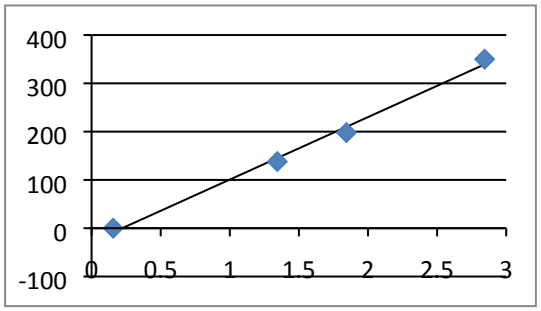

Figure S7: Exemplar calculation of etching rates for silicon and HPC for the Batch (i) (300 W of Fw power and 70 sccm C_4F_8 flow). SEM cross sectional photo shows the depth of the holes transferred in silicon for etching time of 1, 2 and 3 minutes.

Section 5. Additional photos of Al Nanoparticle arrays fabricated with the lift off technique

Aluminum nanoparticles arrays with varying lattice parameter of 400, 500 and 600 nm fabricated with metal deposition and water lift off are shown in **Figure S8**. Prior to depositing the 150 nm Al layer, the samples were etched for 10s using a Reactive Ion Etcher RIE 2000 CE (South Bay Technology Inc.). The etching parameters are 20 sccm of O_2 flow, 5 mTorr pressure and 30 W power and the HPC etching rate is c.a. 160 nm/min. Residual layer thickness of 20 nm was considered for each pattern geometry. Further tuneability of the nanoparticle diameter can be achieved by varying the duration of the etching step that precedes the metal deposition, taking advantage of the lateral erosion that occurs during RIE process (**Figure S9**).

L= 400, etching time 10 s L=500, etching time 10 s L=600 , etching time 10 s

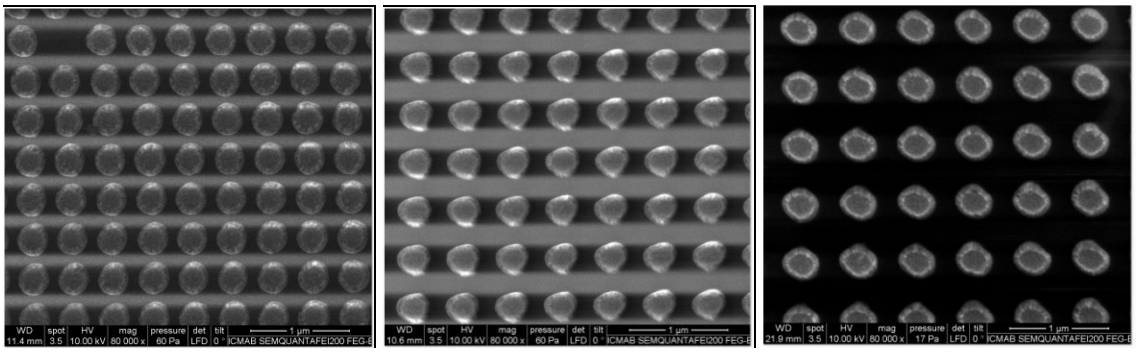

Figure S8: SEM photos of Al nanoparticles arrays with increasing lattice parameter (400, 500 and 600 nm) deposited via metal deposition and lift off.

L= 400, etching time 10 s L=400, etching time 20 s L=400 , etching time 30 s

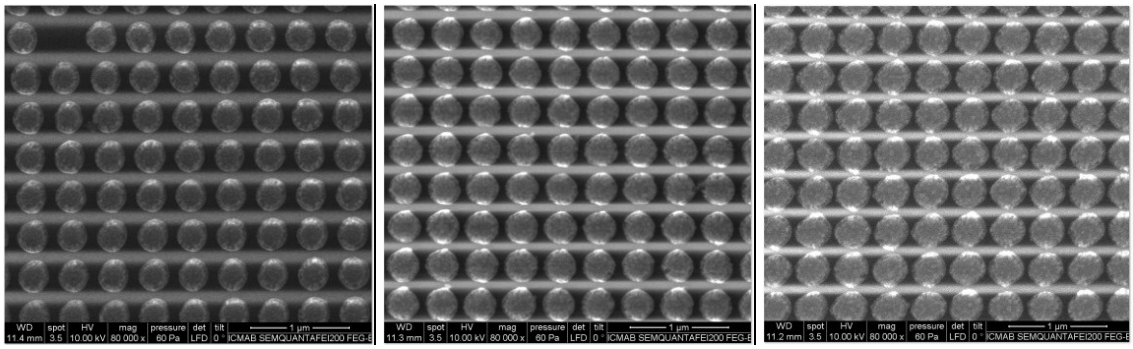

Figure S9: SEM photos of Al nanoparticles arrays with increasing nanoparticles diameter (326, 336 and 356 nm), deposited via metal deposition and lift off.

Section 6. Additional photos of high resolution patterning of Silicon using HPC as resist

Anti reflection patterns (AR) have been successfully transferred to silicon using tNIL and HPC as resist. The AR nanostructures of the master (NIL technology Aps, Denmark) make use of the bio-inspired moth-eye effect, and consist in a hexagonal array of conical shaped pillars (holes), with lattice parameter of 300 nm. Using these structures we could fabricate asymmetrical holes arrays on silicon with minimal dimension of 100 nm (**Figure S10)**. The apparent non-conformity of the HPC pattern in the SEM images is essentially an artifact due to the damage of the HPC pillar during electron scanning.

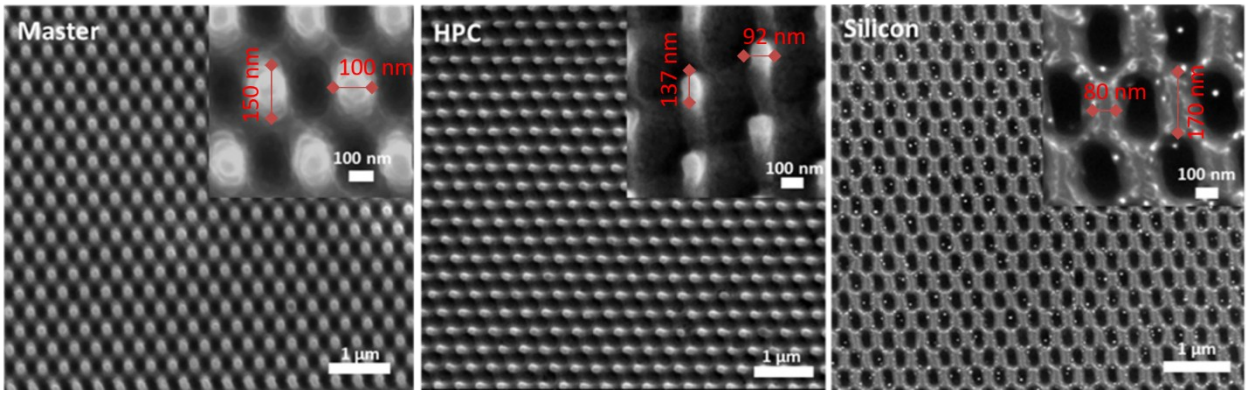

Figure S10: Anti reflection pattern transferred to silicon using HPC as resist. From left to right: SEM top view images of aluminum, imprinted HPC and silicon substrate after RIE.

Section 7. ***Patterning of HPC using electron beam lithography (EBL)***

Hydroxypropyl cellulose was tested under exposure of electron-beam irradiation (SEM FEI InspectF with Raith Elphy add-on) to test its conversion from soluble to insoluble phase. **Fig S11a** shows square patterns after ebeam exposure at different doses and 1 min development in H_2O. The corresponding dose curve extracted from these experiments is summarized in **Fig S12**. The Ideal dose inferred from these results is around 150 µC/cm^2 while lower dose values correspond to an under conversion and higher dose values to an overexposure leading to a thickness decrease. At optimal dose 20% of thickness loss compared to initial cellulose layer thickness is attributed to a swelling of cellulose material.

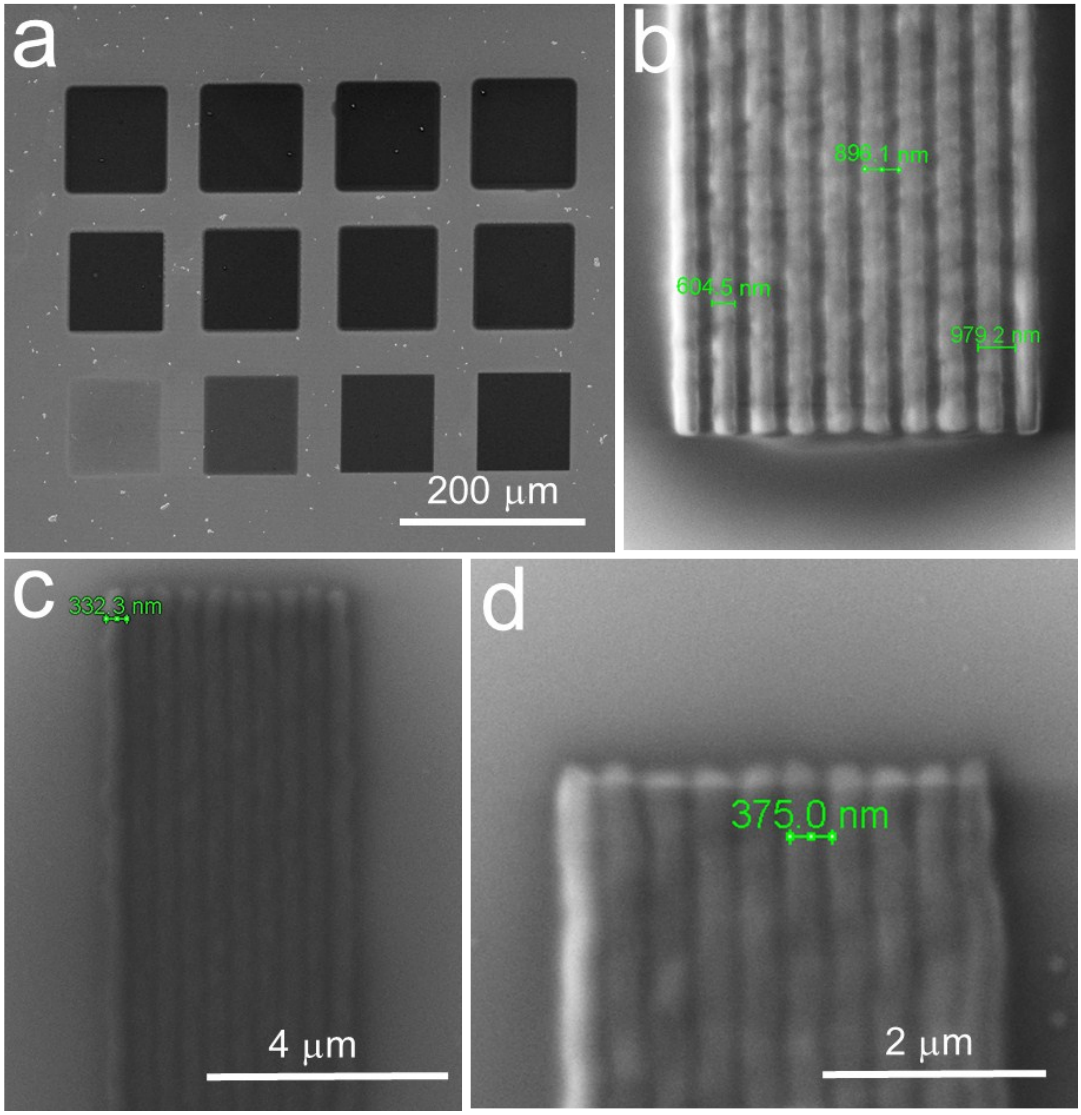

Figure S11 a) Electron beam exposure of cellulose on Si substrate. Dose ranges from 10 to μC/cm^2 to 20500 μC/cm^2, increasing from left to right and from bottom to top. Acceleration voltage of e-beam was 30kV, current 25 pA. b - d) Close up SEM top views of different size e-beam patterned lines in hydroxypropil cellulose .

Fig S12.b –d depicts several SEM images from different size line arrays written with e-beam on cellulose using the optimal conditions. Resolutions as low as 350 nm could be achieved using bare hydroxypropyl cellulose in this preliminar study.

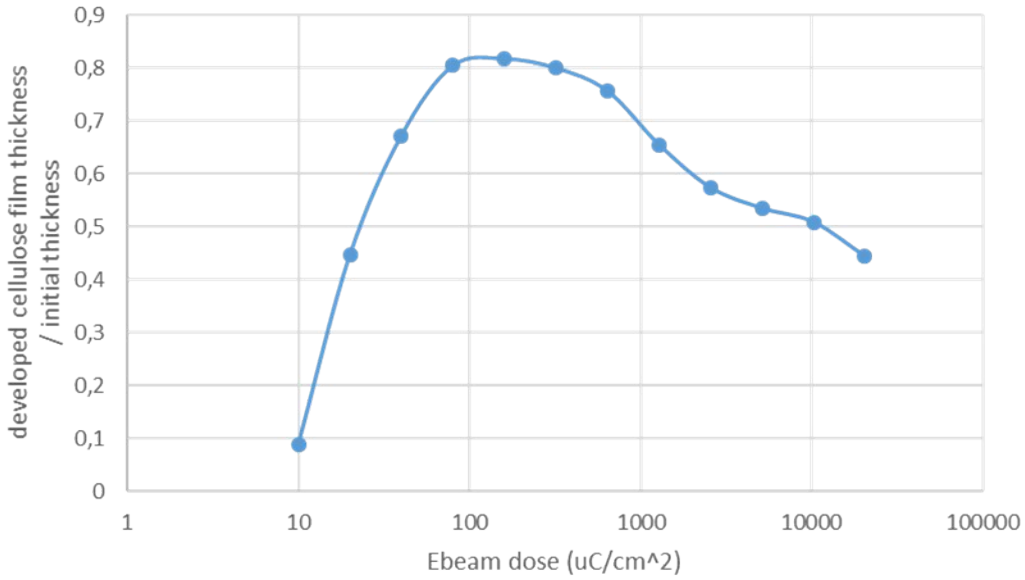

Figure S12: Ratio of the thicknesses of e-beam irradiated structures with initial cellulose layer thickness versus the applied electron beam dose

Comparison of HPC with PVA under EBL patterning

HPC shows much higher sensitivity to electron beam patterning than PVA; the dose required for PVA patterning[4] is at least one order of magnitude higher than the one required for HPC.

[1] P. D. T. Huibers, D. O. Shah, *Langmuir* **1997**, *13*, 5995.

[2] P. Molet, J. L. Garcia-Pomar, C. Matricardi, M. Garriga, M. I. Alonso, A. Mihi, *Advanced materials (Deerfield Beach, Fla.)* **2018**.

[3] D. E. Aspnes, A. A. Studna, *Phys. Rev. B* **1983**, *27*, 985.

[4] José Marqués-Hueso, Rafael Abargues, Josep Canet-Ferrer, Saïd Agouram, José Luís Valdés and Juan P. Martínez-Pastor, *Langmuir*, **2010**, 26 (4), 2825